



# Effects of Chronic Photobiomodulation with Transcranial Near-Infrared Laser on Brain Metabolomics of Young and Aged Rats

Fabrizio dos Santos Cardoso<sup>1,2</sup> · Júlio César Claudino dos Santos<sup>3</sup> · Francisco Gonzalez-Lima<sup>2</sup> · Bruno Henrique Silva Araújo<sup>4</sup> · Rodrigo Álvaro Brandão Lopes-Martins<sup>5</sup> · Sérgio Gomes da Silva<sup>1,6,7</sup>

Received: 23 July 2020 / Accepted: 3 December 2020 / Published online: 8 January 2021  
© The Author(s), under exclusive licence to Springer Science+Business Media, LLC part of Springer Nature 2021

## Abstract

Since laser photobiomodulation has been found to enhance brain energy metabolism and cognition, we conducted the first metabolomics study to systematically analyze the metabolites modified by brain photobiomodulation. Aging is often accompanied by cognitive decline and susceptibility to neurodegeneration, including deficits in brain energy metabolism and increased susceptibility of nerve cells to oxidative stress. Changes in oxidative stress and energetic homeostasis increase neuronal vulnerability, as observed in diseases related to brain aging. We evaluated and compared the cortical and hippocampal metabolic pathways of young (4 months old) and aged (20 months old) control rats with those of rats exposed to transcranial near-infrared laser over 58 consecutive days. Statistical analyses of the brain metabolomics data indicated that chronic transcranial photobiomodulation (1) significantly enhances the metabolic pathways of young rats, particularly for excitatory neurotransmission and oxidative metabolism, and (2) restores the altered metabolic pathways of aged rats towards levels found in younger rats, mainly in the cerebral cortex. These novel metabolomics findings may help complement other laser-induced neurocognitive, neuroprotective, anti-inflammatory, and antioxidant effects described in the literature.

**Keywords** Laser · Photobiomodulation · Brain · Aging · Metabolomics · Metabolic profile

## Introduction

A large number of interventions have been used to modulate metabolic activities. Among them, low-level laser therapy (LLLT), also known as photobiomodulation [1], is well supported in the literature as capable of improving wound healing and reducing pain and inflammation [2–4]. In addition, multiple neurobiological effects of photobiomodulation have been

documented, including studies of the retina [5–7], the spinal cord [8], and the brain [9–13]. For example, in interesting studies with rodents, Oron et al. [14] found beneficial effects using a laser treatment 4 h after brain injury. They reported a restoration of neurological functions such as motor capacity, balance, and alert state, as well as a reduction in brain tissue loss. De Taboada et al. [15] noted that laser treatment improved water maze performance in beta amyloid protein

---

**Highlights** (1) Photobiomodulation increases the brain metabolic pathways of young rats.  
(2) Photobiomodulation restores the brain metabolic pathways of aged rats towards the levels of younger rats.

---

✉ Sérgio Gomes da Silva  
sgomesilva@hotmail.com

- <sup>1</sup> Núcleo de Pesquisas Tecnológicas, Universidade de Mogi das Cruzes, Av. Cândido Xavier de Almeida e Souza, 200, Mogi das Cruzes, SP CEP 08780-911, Brazil
- <sup>2</sup> Department of Psychology and Institute for Neuroscience, University of Texas at Austin, Austin, TX, USA
- <sup>3</sup> Laboratory of Neuroscience, Department of Neurology and Neurosurgery, Federal University of São Paulo, São Paulo, SP, Brazil

- <sup>4</sup> Brazilian Biosciences National Laboratory (LNBio), Brazilian Center for Research in Energy and Materials (CNPEM), Campinas, SP, Brazil
- <sup>5</sup> Laboratory of Biophotonics and Experimental Therapeutics, Institute of Research and Development, University of Vale do Paraíba (UNIVAP), São José dos Campos, SP, Brazil
- <sup>6</sup> Centro Universitário UNIFAMINAS (UNIFAMINAS), Muriaé, MG, Brazil
- <sup>7</sup> Hospital do Câncer de Muriaé, Fundação Cristiano Varella (FCV), Muriaé, MG, Brazil

precursor transgenic mice. They found that enhancement of memory was accompanied by an increase in ATP levels, an improvement in mitochondrial function and greater neuronal activation (c-fos).

Most studies have tested brain photobiomodulation in models of neural lesions or diseases. However, little is known about the beneficial potential of photobiomodulation in the older brain per se [16]. Aging is a progressive multifactorial process, associated with cognitive function impairment and increased susceptibility to neurodegenerative diseases [17]. During aging, there is a decline in energy metabolism, as well as an increased susceptibility of nerve cells to large amounts of oxidative stress [18, 19]. There is also a decrease in the metabolic use of glucose by the cerebral cortex during aging, in humans [20] and rats [21]. During oxidative damage, many molecules such as lipids, carbohydrates, proteins, and DNA are oxidatively modified [17, 22], generating a loss of brain function [23, 24]. These losses related to oxidative stress and energetic homeostasis increase neuronal vulnerability, as observed in diseases related to brain aging [22, 25]. In humans, Vargas et al. [26] investigated transcranial laser effects in older adults, and they found improved cognitive functioning and electroencephalographic rhythms, along with signal reduction in cortical BOLD-fMRI (blood oxygen level dependent-functional magnetic resonance imaging).

Based on these studies, we hypothesized that transcranial photobiomodulation may be beneficial for the metabolic profile of both the young and aged brain. To test this hypothesis, we evaluated whether a chronic transcranial treatment with a laser diode of 810 nm wavelength and 100 mW power has the capacity to alter the cortical and hippocampal metabolic profiles in young and older rats. Metabolomics allows the systematic large-scale study of small molecules called metabolites [27]. To do the metabolomics analysis, we used the analytical technique of nuclear magnetic resonance (NMR) and the MetaboAnalyst platform [28].

## Methods

### Animals

Thirty male Wistar rats, young (4 months old) and aged (20 months old), were used in this study. The colony room was maintained at  $21 \pm 2$  °C with a 12 h light/dark schedule (light: 7 am until 7 pm), and food and water were provided ad libitum throughout the experimental period. All experimental protocols were approved by the ethics committee of the University of Mogi das Cruzes (UMC) (# 016/2017), and all efforts were made to minimize animal suffering in accordance with the proposals of the International Ethical Guideline for Biomedical Research [29].

### Laser Therapy Protocol

The rats were randomly distributed into four groups: young laser (YL;  $n = 7$ ), young control (YC;  $n = 8$ ), aged laser (AL;  $n = 8$ ), and aged control (AC;  $n = 7$ ). One week before the treatment protocol, the animals were adapted daily to the manual handling used for immobilization, which was quick and painless to prevent any discomfort of the animals during the protocol. After this, animals from laser groups (YL and AL) were manually immobilized (without anesthesia) and received the treatment with a laser diode of 810 nm wavelength and 100 mW power for 30 s at each point of application (DMC Equipment, São Carlos, Brazil). We used 5 irradiation points in the skullcap (point 1 = AP + 4.20 mm and ML 0.00 mm; point 2 = AP - 3.00 mm and ML - 6.60 mm; 3 = AP - 3.00 mm and ML + 6.60 mm; point 4 = AP 0.00 mm and ML 0.00 mm; point 5 = AP - 5.52 mm and ML 0.00 mm) (Fig. 1). Thus, the target brain regions were sensory-motor and limbic areas: secondary motor cortex (M2), anterior cingulate cortex (Cga), primary somatosensory cortex-upper limb (S1ULp), secondary somatosensory cortex (S2), posterior cingulate cortex (Cgp), retrosplenial dysgranular cortex (RSD), and retrosplenial granular cortex (RSCg) [30]. The total daily laser treatment was 15 J of energy, 150 s of irradiation, and fluence of  $535.7 \text{ J/cm}^2$ . It is worth mentioning that no difference in scalp temperature measured in the animals was observed with a non-contact thermometer during the treatment protocol. Animals were exposed to the transcranial low-level laser therapy for 58 consecutive days. Animals from control groups (YC and AC) received the same procedure as the laser groups, but as placebo treatment (laser off). The chosen laser parameters listed below were based on our previous publications, which indicated that these parameters had anti-inflammatory properties in different animal models [31–34]. The studies by Morries et al. [35] and Henderson and Morries [36] discuss that in rats, less than 0.5% of energy penetrates the skull and reaches the brain. This means that  $3.5 \text{ W/cm}^2$  on the scalp would represent around  $17 \text{ mW/cm}^2$  in the rat brain. Taken together, the evidence and prior experience give us confidence that the irradiance of our equipment was not harmful to the rat brain. Regarding the number of days of treatment, our rationale was to investigate the therapeutic capacity of chronic treatment with laser.

List of laser parameters:

Center wavelength (nm): 810  
 Operating mode: CW  
 Average radiant power (W): 0.1  
 Aperture diameter (cm): 0.6  
 Irradiance at aperture ( $\text{W/cm}^2$ ): 3.57  
 Beam divergence: near zero  
 Beam shape: circular  
 Beam spot size ( $\text{cm}^2$ ): 0.028

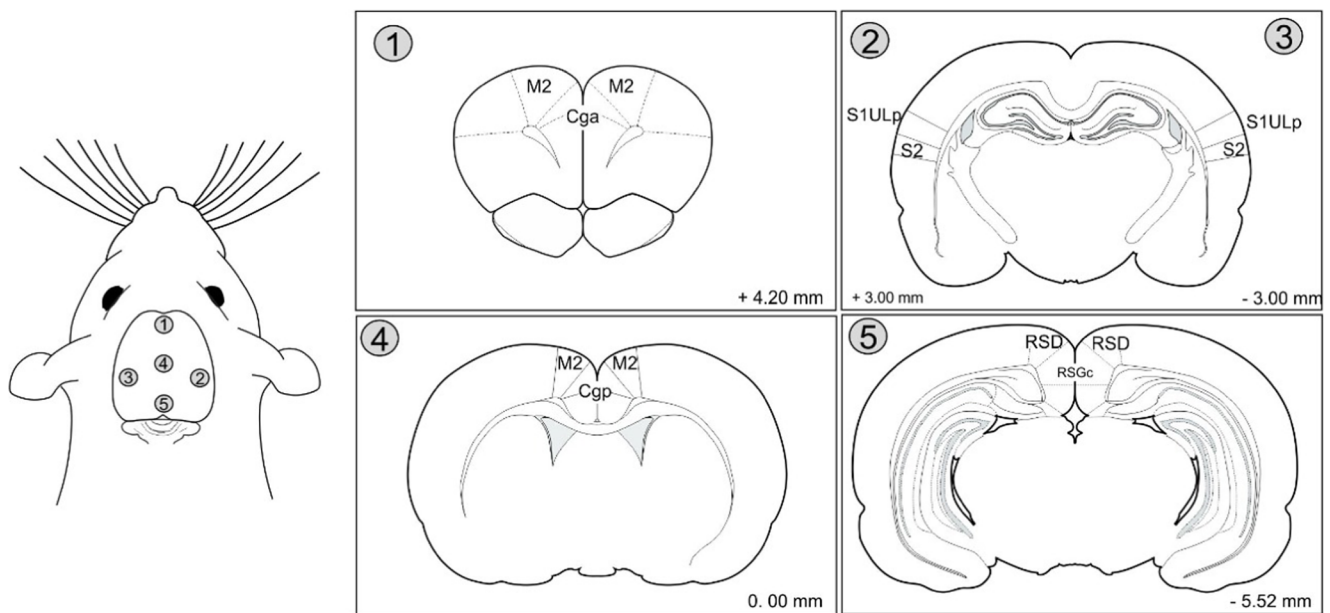


**Fig. 1** Five irradiation points over the scalp (target coordinates: point 1 = AP + 4.20 mm, ML 0.00 mm; point 2 = AP - 3.00 mm, ML - 6.60 mm; point 3 = AP - 3.00 mm, ML + 6.60 mm; point 4 = AP 0.00 mm, ML 0.00 mm; point 5 = AP - 5.52 mm, ML 0.00 mm). Abbreviations:

secondary motor cortex (M2), anterior cingulate cortex (Cga), primary somatosensory cortex-upper limb (S1ULp), secondary somatosensory cortex (S2), posterior cingulate cortex (Cgp), retrosplenial dysgranular cortex (RSD), and retrosplenial granular cortex (RSGc)

Exposure duration/point (s): 30  
 Radiant exposure ( $J/cm^2$ ) per point per session: 107.14  
 Number of points irradiated: five  
 Delivery mode: contact mode  
 Number and frequency of sessions: one session/day for 58 consecutive days.  
 Total radiant energy (J) per head: 15

## Metabolomics Profile

Twenty-four hours after the last laser therapy session, animals were euthanized by decapitation. Immediately after decapitation, the cerebral cortex and hippocampal formation (Ammon's horn and dentate gyrus) of the YL ( $n = 7$ ), YC ( $n = 8$ ), AL ( $n = 8$ ), and AC ( $n = 7$ ) groups were dissected by means of consistent anatomical landmarks and maintained at  $-80\text{ }^\circ\text{C}$  for analysis of the metabolomics profile. Brain tissue was pulverized using ceramic mortar and pestle under liquid nitrogen. For the extraction procedure, approximately 30 mg of the pulverized material was weighed, and 334  $\mu\text{L}$  of methanol and 166  $\mu\text{L}$  of chloroform (2:1, v/v) were added. The solution was mixed in a vortex for 10 s and sonicated for 5 min. Then, a sample was kept for  $\sim 15$  min in ice bath. Thereafter, 250  $\mu\text{L}$  of chloroform and 250  $\mu\text{L}$  of Milli-Q water (1:1, v/v) were added, followed by mixing in a vortex for 10 s and centrifugation at 14,000 rpm at  $4\text{ }^\circ\text{C}$  for 20 min, for subsequent supernatant fraction collection. The procedure was repeated with the precipitated fraction of the supernatant.

After this procedure, the supernatant fractions were mixed ( $\sim 0.8$  mL), dried using speed vac (MIVAC DUO) and kept at  $-80\text{ }^\circ\text{C}$ . For NMR acquisitions, a sample was solubilized in 540  $\mu\text{L}$  of deuterium oxide ( $\text{D}_2\text{O}$ , 99.9%; Cambridge Isotope Laboratories Inc., MA, USA), 60  $\mu\text{L}$  phosphate buffer (0.1 M, pH 7.4), and 0.5 mM TMSP- $d_4$  (3-(trimethylsilyl)-2,2',3,3'-tetradeuteriopropionic acid, Sigma-Aldrich) to produce a final 0.6 mL solution and then transferred to a 5 mm NMR tube (Norell Standard Series 5 mm, Sigma-Aldrich) for immediate data acquisition.

## NMR Acquisition Spectra

The  $^1\text{H}$  NMR spectra of the samples were acquired using an Agilent Inova 600 spectrometer (Agilent Technologies Inc.<sup>TM</sup>, Santa Clara, USA) from the Brazilian Biosciences National Laboratory (Brazilian Center for Research in Energy and Materials (CNPEM)) equipped with a triple resonance cryoprobe and operating at a  $^1\text{H}$  resonance frequency of 599.887 MHz and constant temperature of 298 K ( $25\text{ }^\circ\text{C}$ ). A total of 256 or 512 free induction decays, depending on the concentration of metabolites, were collected with 32 k data points at a spectral width of 16 ppm and acquisition time of 4 s. A relaxation delay of 1.5 s was incorporated between the scans, during which a continuous pre-saturation radiofrequency (RF) field of water was applied.

NMR spectroscopy is a useful technique for identifying and determining the structure of biomolecules such as proteins and nucleic acids. This technique is dependent on

concentration (usually mg of compounds) and molecular weight. Using the most common  $^1\text{H}$  NMR spectroscopy, it is possible to identify most chemicals that contain hydrogens in their structure. In the NMR spectra, the area under each hydrogen sign represents the concentration and number of hydrogen atoms of a given compound, and the chemical shifts (ppm) are the resonance frequency of each atom, depending on the chemical environment in which they are found. On the same conditions (such as pH and temperature), the NMR spectra are very reproducible, so we can use the information on chemical shifts, multiplicity, J coupling, etc., to identify a compound if the spectrum is equal to a spectrum of reference.

### Identification and Quantification of Metabolites

Data preprocessing, spectral phase, and baseline corrections, as well as the identification and quantification of metabolites present in samples, were performed using Chenomx NMR Suite 8.1 software (Chenomx Inc.<sup>TM</sup>, Edmonton, Canada). The Chenomx NMR Analysis Software is designed to use the Spectral Reference Library to select the appropriate signals within the experimental spectrum. The software automatically configures the Reference Library to reproduce the sample. In summary, we detected 48 metabolites in the cortex (Table 1) and 48 metabolites in the hippocampus (Table 2) with sufficient signal-to-noise ratios.

### Statistical Analyses

For exploratory analysis, we used principal component analysis (PCA), a non-supervised exploratory statistical tool that detects the variables responsible for the greater variance between the data. In this analysis, the samples are grouped according to their similarity, without prior information on the groups studied. In the PCA, two types of plots are generated, the score plot and the loading plot, which necessarily need to be analyzed together. The score plot provides the coordinates of the samples, while the loading plot shows the contribution of the variables in the construction of the main components.

After this, the Z-score was used to remove outlier values. The statistical procedures for hypothesis testing were conducted with the four groups simultaneously by two-way ANOVA followed by post hoc tests with the Bonferroni correction. The analyses were performed using the Statistical Package for the Social Sciences (SPSS Inc., IBM, version 22.0, Chicago, USA). A statistical difference was considered significant with a value of  $p < 0.05$ .

For metabolic pathway analysis, we used metabolite set enrichment analysis (MSEA) to identify metabolic pathways possibly altered by differences in metabolite concentrations found between groups. The analyses were performed using the MetaboAnalyst platform [28].

## Results

### Cortical Metabolomics Profile

We used the exploratory PCA test to analyze the characteristics of the groups, and the ANOVA hypothesis testing was performed to detect the differences between the groups. The statistical results of the two-way ANOVA of the cortical data are presented in Supplementary Table 1.

When the corrected post hoc analysis of Bonferroni was performed, no significant difference in the metabolites adenine, creatine phosphate, and tryptophan ( $p > 0.05$ ) was observed between the AC and YC groups. However, in the other metabolites investigated, the AC group exhibited a higher concentration in relation to the YC group ( $p < 0.05$ ) (Table 1).

In young rats, the laser treatment significantly increased the concentration of 4-aminobutyrate, AMP, acetate, alanine, ascorbate, aspartate, betaine, choline, creatine, creatine phosphate, creatinine, formate, fumarate, GTP, glutamate, glutamine, glutathione, glycerol, glycine, lactate, lysine, N-acetyl-L-aspartate, O-phosphoethanolamine, oxypurinol, phenylalanine, taurine, threonine, tyrosine, uridine, myo-inositol, sn-glycero-3-phosphocholine, and 3-methylhistidine (YC vs YL;  $p < 0.05$ ) (Table 1).

In addition, the laser reversed the high concentration of these metabolites observed in aged rats (AC vs AL;  $p < 0.05$ ). Only the metabolites adenine and tryptophan were not significantly reduced by photobiomodulation ( $p > 0.05$ ) (Table 1). Taken together, these data showed that the photobiomodulation was able to alter the cortical metabolic profile of young and aged rats.

A similarity was observed between the YC, YL, and AL groups when using PCA. A complete distinction of the data was noted between AC and other groups (Fig. 2a). In addition, the variables responsible for the difference in the score plot were found in the loading plot (Fig. 2b). Together, the two principal components selected by the analysis accounted for 87.7% of the data variance.

### Cortical Metabolic Pathways Altered by Aging in Control Rats

After observing the differences between the groups, it was possible to analyze and interpret the impacted metabolic pathways through the metabolite set enrichment analysis (MSEA). This analysis was performed with metabolites that exhibited significant changes among studied groups.

When we analyzed the cortical metabolic pathways altered by aging (AC vs YC), we observed a significant increase in the pathways of aspartate metabolism ( $p < 0.0001$ ), glutamate metabolism ( $p = 0.001$ ), ammonia recycling ( $p = 0.001$ ), urea cycle ( $p = 0.003$ ), purine

**Table 1** Concentration of cortical metabolites ( $\mu\text{M}$ ) in YC ( $n = 8$ ), YL ( $n = 7$ ), AC ( $n = 7$ ), and AL ( $n = 8$ ) groups

Metabolite ( $\mu\text{M}$ )	YC	YL	AC	AL
4-Aminobutyrate	710.9 $\pm$ 83.7	1503.0 $\pm$ 155.9 <sup>a</sup>	5128.2 $\pm$ 293.1 <sup>b</sup>	2136.8 $\pm$ 113.3 <sup>c</sup>
4-Pyridoxate	27.2 $\pm$ 5.0	31.2 $\pm$ 4.1	225.5 $\pm$ 19.7 <sup>b</sup>	95.4 $\pm$ 14.7 <sup>c</sup>
AMP	83.4 $\pm$ 12.8	217.3 $\pm$ 16.8 <sup>a</sup>	469.4 $\pm$ 52.5 <sup>b</sup>	190.9 $\pm$ 24.1 <sup>c</sup>
ATP	14.5 $\pm$ 2.4	32.7 $\pm$ 9.4	162.3 $\pm$ 22.9 <sup>b</sup>	54.4 $\pm$ 11.8 <sup>c</sup>
Acetate	178.1 $\pm$ 29.8	466.4 $\pm$ 83.0 <sup>a</sup>	800.1 $\pm$ 40.8 <sup>b</sup>	403.8 $\pm$ 32.5 <sup>c</sup>
Adenine	37.4 $\pm$ 6.2	35.4 $\pm$ 10.4	53.8 $\pm$ 10.7	47.2 $\pm$ 17.4
Adenosine	141.4 $\pm$ 13.7	244.7 $\pm$ 32.1	1022.1 $\pm$ 78.1 <sup>b</sup>	386.8 $\pm$ 28.6 <sup>c</sup>
Alanine	275.0 $\pm$ 37.4	553.9 $\pm$ 51.2 <sup>a</sup>	1641.5 $\pm$ 106.9 <sup>b</sup>	706.7 $\pm$ 23.1 <sup>c</sup>
Ascorbate	501.5 $\pm$ 132.0	1316.9 $\pm$ 194.7 <sup>a</sup>	3313.8 $\pm$ 322.8 <sup>b</sup>	1775.4 $\pm$ 90.3 <sup>c</sup>
Asparagine	33.7 $\pm$ 3.3	61.5 $\pm$ 10.4	282.9 $\pm$ 27.3 <sup>b</sup>	95.4 $\pm$ 4.8 <sup>c</sup>
Aspartate	1023.5 $\pm$ 135.7	2156.4 $\pm$ 202.1 <sup>a</sup>	6353.3 $\pm$ 484.7 <sup>b</sup>	2829.9 $\pm$ 110.4 <sup>c</sup>
Betaine	15.2 $\pm$ 1.3	33.9 $\pm$ 3.3 <sup>a</sup>	85.3 $\pm$ 6.2 <sup>b</sup>	39.3 $\pm$ 3.7 <sup>c</sup>
Choline	158.1 $\pm$ 17.9	301.8 $\pm$ 36.3 <sup>a</sup>	887.7 $\pm$ 76.6 <sup>b</sup>	372.6 $\pm$ 35.0 <sup>c</sup>
Creatine	3088.0 $\pm$ 445.8	6407.2 $\pm$ 645.4 <sup>a</sup>	20,419.0 $\pm$ 1114.3 <sup>b</sup>	8907.9 $\pm$ 382.0 <sup>c</sup>
Creatine phosphate	58.9 $\pm$ 11.4	34.1 $\pm$ 5.4 <sup>a</sup>	61.3 $\pm$ 5.5	39.1 $\pm$ 3.9 <sup>c</sup>
Creatinine	33.5 $\pm$ 4.7	55.1 $\pm$ 4.0 <sup>a</sup>	73.4 $\pm$ 5.3 <sup>b</sup>	28.9 $\pm$ 2.1 <sup>c</sup>
Ethanol	386.1 $\pm$ 28.7	344.0 $\pm$ 29.8	1522.5 $\pm$ 138.8 <sup>b</sup>	456.0 $\pm$ 38.6 <sup>c</sup>
Formate	51.4 $\pm$ 7.4	119.3 $\pm$ 13.7 <sup>a</sup>	229.9 $\pm$ 14.5 <sup>b</sup>	82.3 $\pm$ 2.7 <sup>c</sup>
Fumarate	33.1 $\pm$ 4.5	56.6 $\pm$ 3.3 <sup>a</sup>	233.8 $\pm$ 11.7 <sup>b</sup>	97.0 $\pm$ 5.8 <sup>c</sup>
GTP	28.5 $\pm$ 4.6	61.7 $\pm$ 9.5 <sup>a</sup>	193.0 $\pm$ 16.5 <sup>b</sup>	106.8 $\pm$ 6.7 <sup>c</sup>
Glutamate	3794.0 $\pm$ 511.9	7891.2 $\pm$ 836.1 <sup>a</sup>	21,993.3 $\pm$ 1322.0 <sup>b</sup>	9555.1 $\pm$ 426.8 <sup>c</sup>
Glutamine	1540.3 $\pm$ 239.4	3289.6 $\pm$ 390.7 <sup>a</sup>	10,367.7 $\pm$ 479.7 <sup>b</sup>	4833.5 $\pm$ 396.1 <sup>c</sup>
Glutathione	108.8 $\pm$ 23.5	397.1 $\pm$ 80.5 <sup>a</sup>	1204.0 $\pm$ 52.4 <sup>b</sup>	481.8 $\pm$ 42.4 <sup>c</sup>
Glycerol	239.6 $\pm$ 32.9	358.4 $\pm$ 27.3 <sup>a</sup>	1015.4 $\pm$ 47.8 <sup>b</sup>	477.3 $\pm$ 34.3 <sup>c</sup>
Glycine	295.1 $\pm$ 41.6	605.4 $\pm$ 52.2 <sup>a</sup>	1923.9 $\pm$ 77.8 <sup>b</sup>	824.7 $\pm$ 46.9 <sup>c</sup>
Histidine	17.5 $\pm$ 2.9	31.0 $\pm$ 4.1	96.3 $\pm$ 8.2 <sup>b</sup>	43.3 $\pm$ 3.2 <sup>c</sup>
Hypoxanthine	86.2 $\pm$ 11.6	144.3 $\pm$ 14.6	621.1 $\pm$ 14.8 <sup>b</sup>	264.2 $\pm$ 37.6 <sup>c</sup>
Inosine	116.1 $\pm$ 14.6	183.2 $\pm$ 16.4	1053.4 $\pm$ 84.4 <sup>b</sup>	412.9 $\pm$ 85.4 <sup>c</sup>
Isoleucine	23.5 $\pm$ 3.3	29.4 $\pm$ 4.0	93.9 $\pm$ 7.1 <sup>b</sup>	42.2 $\pm$ 3.9 <sup>c</sup>
Lactate	3619.8 $\pm$ 532.6	7268.6 $\pm$ 704.2 <sup>a</sup>	25,842.5 $\pm$ 646.1 <sup>b</sup>	11,726.5 $\pm$ 519.6 <sup>c</sup>
Leucine	42.2 $\pm$ 2.4	64.6 $\pm$ 7.7	203.5 $\pm$ 15.0 <sup>b</sup>	90.3 $\pm$ 8.9 <sup>c</sup>
Lysine	56.3 $\pm$ 5.1	112.1 $\pm$ 10.0 <sup>a</sup>	274.1 $\pm$ 21.3 <sup>b</sup>	138.2 $\pm$ 13.5 <sup>c</sup>
N-Acetyl-L-aspartate	2890.2 $\pm$ 430.1	6211.4 $\pm$ 606.8 <sup>a</sup>	18,426.4 $\pm$ 1127.2 <sup>b</sup>	8273.9 $\pm$ 345.4 <sup>c</sup>
Niacinamide	84.4 $\pm$ 11.0	140.2 $\pm$ 21.3	475.2 $\pm$ 33.4 <sup>b</sup>	210.8 $\pm$ 12.2 <sup>c</sup>
O-Phosphocholine	87.2 $\pm$ 13.9	160.0 $\pm$ 13.3	543.2 $\pm$ 43.3 <sup>b</sup>	210.9 $\pm$ 8.3 <sup>c</sup>
O-Phosphoethanolamine	527.5 $\pm$ 65.1	1095.6 $\pm$ 114.3 <sup>a</sup>	3247.3 $\pm$ 198.3 <sup>b</sup>	1274.5 $\pm$ 40.6 <sup>c</sup>
Oxypurinol	912.2 $\pm$ 118.2	2074.5 $\pm$ 138.4 <sup>a</sup>	5036.6 $\pm$ 529.3 <sup>b</sup>	2225.0 $\pm$ 293.1 <sup>c</sup>
Phenylalanine	16.7 $\pm$ 1.2	34.9 $\pm$ 3.3 <sup>a</sup>	102.4 $\pm$ 7.1 <sup>b</sup>	45.3 $\pm$ 3.6 <sup>c</sup>
Succinate	56.1 $\pm$ 7.8	119.7 $\pm$ 27.7	287.6 $\pm$ 42.9 <sup>b</sup>	120.0 $\pm$ 21.6 <sup>c</sup>
Taurine	1833.2 $\pm$ 267.0	3819.3 $\pm$ 452.8 <sup>a</sup>	10,880.9 $\pm$ 502.6 <sup>b</sup>	4580.1 $\pm$ 181.6 <sup>c</sup>
Threonine	178.8 $\pm$ 23.0	334.2 $\pm$ 36.4 <sup>a</sup>	1140.5 $\pm$ 64.0 <sup>b</sup>	448.6 $\pm$ 44.1 <sup>c</sup>
Tryptophan	15.6 $\pm$ 1.4	20.2 $\pm$ 2.5	29.7 $\pm$ 8.1	15.5 $\pm$ 3.2
Tyrosine	24.7 $\pm$ 2.6	51.1 $\pm$ 7.0 <sup>a</sup>	148.5 $\pm$ 3.3 <sup>b</sup>	66.2 $\pm$ 8.3 <sup>c</sup>
Uridine	25.0 $\pm$ 3.7	53.1 $\pm$ 8.7 <sup>a</sup>	177.8 $\pm$ 15.8 <sup>b</sup>	73.5 $\pm$ 4.0 <sup>c</sup>
Valine	40.8 $\pm$ 4.8	60.7 $\pm$ 3.6	207.0 $\pm$ 12.4 <sup>b</sup>	91.8 $\pm$ 5.0 <sup>c</sup>
Myo-Inositol	1725.4 $\pm$ 239.3	3572.7 $\pm$ 371.2 <sup>a</sup>	12,378.6 $\pm$ 609.1 <sup>b</sup>	5059.9 $\pm$ 110.2 <sup>c</sup>
sn-Glycero-3-phosphocholine	162.0 $\pm$ 22.1	353.3 $\pm$ 63.9 <sup>a</sup>	1087.0 $\pm$ 63.6 <sup>b</sup>	437.4 $\pm$ 64.2 <sup>c</sup>
3-Methylhistidine	25.8 $\pm$ 2.7	49.8 $\pm$ 7.4 <sup>a</sup>	147.9 $\pm$ 5.4 <sup>b</sup>	59.4 $\pm$ 4.2 <sup>c</sup>

<sup>a</sup> Difference between YL vs YC groups<sup>b</sup> Difference between AC vs YC groups<sup>c</sup> Difference between AL vs AC groups; ( $p < 0.05$ ; two-way ANOVA, followed by the Bonferroni post hoc analysis)

metabolism ( $p = 0.003$ ), alanine metabolism ( $p = 0.008$ ), phenylalanine and tyrosine metabolism ( $p = 0.013$ ), arginine and proline metabolism ( $p = 0.017$ ), glutathione metabolism ( $p = 0.017$ ), phosphatidylcholine biosynthesis ( $p = 0.023$ ), glycine and serine metabolism ( $p = 0.026$ ), and phenylacetate metabolism ( $p = 0.045$ ).

### Cortical Metabolic Pathways Altered by Photobiomodulation in Young Rats

The cortical metabolic pathways increased by photobiomodulation in young rats (YC vs YL) were aspartate metabolism ( $p < 0.0001$ ), glutamate metabolism ( $p = 0.003$ ),



urea cycle ( $p = 0.005$ ), arginine and proline metabolism ( $p = 0.020$ ), phenylalanine and tyrosine metabolism ( $p = 0.022$ ), alanine metabolism ( $p = 0.022$ ), glycine and serine metabolism ( $p = 0.022$ ), ammonia recycling ( $p = 0.029$ ), and glutathione metabolism ( $p = 0.035$ ) (Fig. 3).

### Cortical Metabolic Pathways Altered by Photobiomodulation in Aged Rats

The cortical metabolic pathways decreased by photobiomodulation in aged rats (AC vs AL) were aspartate metabolism ( $p < 0.0001$ ), glutamate metabolism ( $p = 0.001$ ), ammonia recycling ( $p = 0.001$ ), urea cycle ( $p = 0.004$ ), purine metabolism ( $p = 0.005$ ), arginine and proline metabolism ( $p = 0.006$ ), alanine metabolism ( $p = 0.009$ ), phenylalanine and tyrosine metabolism ( $p = 0.014$ ), glutathione metabolism ( $p = 0.020$ ), phosphatidylcholine biosynthesis ( $p = 0.027$ ), and glycine and serine metabolism ( $p = 0.035$ ) (Fig. 4).

### Hippocampal Metabolomics Profile

The statistical results of the two-way ANOVA of the hippocampal data are presented in Supplementary Table 2. When the corrected post hoc analysis of Bonferroni was performed, the AC group showed a lower concentration of acetate when compared to the YC group ( $p = 0.044$ ). In addition, photobiomodulation increased the concentration of acetate ( $p = 0.038$ ) and guanosine triphosphate (GTP) ( $p = 0.002$ ) of aged rats (Table 2). We could not perform further analyses of the hippocampal metabolic pathways because we observed differences in only two of the metabolites, acetate and GTP.

The hippocampus PCA is shown in Fig. 5. A similarity between the control (YC and AC) and laser (YL and AL) groups was observed (Fig. 5a). In addition, we found in the loading plot the variables responsible for the difference in the score plot (Fig. 5b). Together, the two principal components selected by the analysis accounted for 78% of the data variance.

## Discussion

The purpose of this study was to investigate the effects of transcranial photobiomodulation on the cortical and hippocampal metabolic profiles of rats with 4 or 20 months of age exposed to a chronic treatment with a laser of 810 nm wavelength and 100 mW power. The power density/irradiance used was high due to the very small spot size of the laser equipment aperture ( $0.028 \text{ cm}^2$ ), which give us  $3.57 \text{ W/cm}^2$ . However, the irradiation time consisted of 30 s/point in 5 different points. This means that the total time of irradiation of 150 s was divided into five points, as shown in Fig. 1. Due to our previous

experience with this equipment and such doses, we should say that this dose does not induce any kind of hazard to the biological tissues. The chosen laser parameters were already used in more than 50 publications from our group, studying the anti-inflammatory properties and mechanisms of laser therapy in different animal models (e.g., [31–34]).

### Photobiomodulation Increases the Brain Metabolic Pathways of Young Rats

In the young rats, transcranial photobiomodulation increased the metabolic pathways of alanine, aspartate, arginine, glutamate, glutathione, glycine, phenylalanine, proline, serine, and tyrosine in the cerebral cortex. These laser-induced metabolic effects are promising because these molecules play an important role in neuronal activity [37–40]. Aspartate and glutamate, for instance, are the main excitatory neurotransmitters of the mammalian brain, playing important roles in neuronal development, synaptic plasticity, and in learning and memory [39, 40]. Proline, in turn, is capable of activating NMDA receptors [41–44], modulating the neurotransmission of glutamate. In young humans, transcranial photobiomodulation can modulate cortical excitability [45] and cortical electrical rhythms [13]. Glutathione plays a pivotal role in the cellular antioxidant system [46], besides regulating other cellular events, such as gene expression, DNA synthesis, cellular proliferation, and apoptosis [47]. Moreover, an increase in the phenylalanine pathway may contribute to dopamine neurotransmission in the prefrontal cortex, which improves cognitive functions [48], while its depletion results in dopamine reduction and cognitive impairment [27, 48, 49]. In young humans, transcranial photobiomodulation enhances cognitive functions [50]. Thus, the cortical metabolic profile induced by transcranial photobiomodulation could be beneficial to the young brain.

A primary mechanism of action of transcranial photobiomodulation is the induction of cytochrome-c-oxidase, the main intracellular photon acceptor in the red-to-near-infrared wavelengths, which has been demonstrated to facilitate cortical oxidative metabolism in rats [51] and humans [12]. Photobiomodulation of cytochrome-c-oxidase activity is consistent with the observed cortical metabolic profiles found in this study. For example, induction of the transcription of cytochrome-c-oxidase subunits is associated to glutamatergic receptor activation because there is a coupling of cytochrome-c-oxidase genes with excitatory neurotransmission genes at the transcriptional level [52]. All ten nuclear genes and the three mitochondrial transcription factors of cytochrome-c-oxidase are transcribed in the same “transcription factory” as the

**Table 2** Concentration of hippocampal metabolites ( $\mu\text{M}$ ) in YC ( $n = 7$ ), YL ( $n = 7$ ), AC ( $n = 6$ ), and AL ( $n = 8$ ) groups

Metabolite ( $\mu\text{M}$ )	YC	YL	AC	AL
4-Aminobutyrate	2280.6 $\pm$ 315.8	1400.4 $\pm$ 262.8	2179.3 $\pm$ 328.0	1570.4 $\pm$ 281.6
4-Pyridoxate	48.6 $\pm$ 7.2	19.6 $\pm$ 3.5	73.8 $\pm$ 8.1	22.4 $\pm$ 13.5
AMP	19.0 $\pm$ 5.4	104.5 $\pm$ 22.6	29.1 $\pm$ 8.2	109.0 $\pm$ 21.3
ATP	6.3 $\pm$ 1.6	18.6 $\pm$ 3.4	9.0 $\pm$ 0.7	20.7 $\pm$ 3.6
Acetate	262.1 $\pm$ 75.2	121.2 $\pm$ 39.8	85.2 $\pm$ 9.9 <sup>b</sup>	263.6 $\pm$ 52.4 <sup>c</sup>
Adenine	6.1 $\pm$ 0.5	5.5 $\pm$ 1.4	5.2 $\pm$ 0.9	3.6 $\pm$ 0.2
Adenosine	10.9 $\pm$ 1.5	328.4 $\pm$ 62.9	14.2 $\pm$ 2.8	439.2 $\pm$ 93.1
Alanine	574.3 $\pm$ 74.7	596.8 $\pm$ 121.3	588.2 $\pm$ 74.3	602.6 $\pm$ 113.1
Ascorbate	425.9 $\pm$ 134.6	1200.1 $\pm$ 338.5	701.9 $\pm$ 143.6	1227.2 $\pm$ 324.3
Asparagine	69.9 $\pm$ 14.9	54.1 $\pm$ 14.4	68.8 $\pm$ 10.4	83.5 $\pm$ 29.4
Aspartate	1506.3 $\pm$ 185.7	1073.7 $\pm$ 212.1	1586.5 $\pm$ 197.9	1209.6 $\pm$ 256.2
Betaine	32.4 $\pm$ 4.5	31.1 $\pm$ 4.7	26.5 $\pm$ 3.1	32.8 $\pm$ 5.0
Butyrate	49.1 $\pm$ 6.3	45.4 $\pm$ 10.0	22.2 $\pm$ 6.1	18.1 $\pm$ 5.0
Choline	357.6 $\pm$ 48.6	192.3 $\pm$ 32.8	358.0 $\pm$ 52.7	210.9 $\pm$ 32.2
Creatine	4603.3 $\pm$ 594.3	5326.5 $\pm$ 1026.1	5299.3 $\pm$ 667.1	5690.0 $\pm$ 1090.6
Creatine phosphate	35.7 $\pm$ 3.9	31.1 $\pm$ 4.9	23.5 $\pm$ 2.4	32.6 $\pm$ 6.1
Creatinine	71.5 $\pm$ 6.5	61.4 $\pm$ 11.6	20.8 $\pm$ 3.1	37.5 $\pm$ 12.3
Ethanol	424.6 $\pm$ 17.0	349.9 $\pm$ 41.7	718.8 $\pm$ 73.7	771.9 $\pm$ 51.0
Formate	108.4 $\pm$ 16.6	73.8 $\pm$ 17.2	84.7 $\pm$ 8.5	54.1 $\pm$ 6.3
Fumarate	44.8 $\pm$ 6.1	44.7 $\pm$ 8.5	52.4 $\pm$ 5.7	57.3 $\pm$ 9.8
GTP	18.6 $\pm$ 3.9	15.2 $\pm$ 4.3	26.9 $\pm$ 7.4	77.1 $\pm$ 15.8 <sup>c</sup>
Glutamate	3957.6 $\pm$ 533.2	5732.1 $\pm$ 1126.3	4768.4 $\pm$ 588.3	5806.8 $\pm$ 1170.6
Glutamine	2256.9 $\pm$ 271.5	2557.6 $\pm$ 462.0	2747.4 $\pm$ 354.6	3309.9 $\pm$ 871.6
Glutathione	49.1 $\pm$ 8.6	242.6 $\pm$ 74.0	72.8 $\pm$ 11.1	383.1 $\pm$ 95.7
Glycerol	366.3 $\pm$ 37.8	279.8 $\pm$ 55.8	349.2 $\pm$ 40.2	311.4 $\pm$ 57.7
Glycine	856.8 $\pm$ 114.7	579.8 $\pm$ 110.0	894.0 $\pm$ 123.1	661.3 $\pm$ 131.7
Histidine	27.5 $\pm$ 5.7	22.3 $\pm$ 4.7	29.9 $\pm$ 4.9	34.5 $\pm$ 9.5
Hypoxanthine	521.0 $\pm$ 61.3	114.5 $\pm$ 17.0	450.5 $\pm$ 73.0	128.8 $\pm$ 25.6
Inosine	393.7 $\pm$ 58.2	136.6 $\pm$ 19.5	513.9 $\pm$ 68.1	167.6 $\pm$ 34.2
Isoleucine	34.6 $\pm$ 4.2	27.5 $\pm$ 5.8	37.0 $\pm$ 3.7	29.1 $\pm$ 6.1
Lactate	6225.0 $\pm$ 1059.1	6281.9 $\pm$ 1477.5	8096.0 $\pm$ 1162.9	8964.1 $\pm$ 1779.5
Leucine	87.0 $\pm$ 10.2	56.0 $\pm$ 9.5	73.2 $\pm$ 11.6	75.2 $\pm$ 15.1
Lysine	146.9 $\pm$ 20.7	75.3 $\pm$ 13.5	110.9 $\pm$ 17.8	110.8 $\pm$ 29.1
N-Acetyl-L-aspartate	3484.4 $\pm$ 469.1	3988.8 $\pm$ 763.8	4027.0 $\pm$ 486.4	4527.8 $\pm$ 843.4
Niacinamide	98.3 $\pm$ 14.9	88.6 $\pm$ 25.1	90.7 $\pm$ 21.0	129.4 $\pm$ 34.0
O-Phosphocholine	239.2 $\pm$ 32.5	212.3 $\pm$ 41.2	221.8 $\pm$ 29.2	206.2 $\pm$ 38.3
O-Phosphoethanolamine	803.5 $\pm$ 101.0	753.5 $\pm$ 152.1	786.1 $\pm$ 99.9	989.6 $\pm$ 194.4
Oxypurinol	249.4 $\pm$ 77.7	1066.2 $\pm$ 227.3	488.3 $\pm$ 95.5	1108.8 $\pm$ 236.5
Phenylalanine	34.4 $\pm$ 4.7	25.5 $\pm$ 5.4	38.5 $\pm$ 3.6	30.3 $\pm$ 9.5
Succinate	46.2 $\pm$ 2.1	58.1 $\pm$ 10.7	45.8 $\pm$ 4.2	49.9 $\pm$ 7.3
Taurine	2837.1 $\pm$ 396.9	3374.8 $\pm$ 675.1	3147.5 $\pm$ 377.1	3619.7 $\pm$ 728.9
Threonine	264.6 $\pm$ 40.2	239.4 $\pm$ 58.5	291.4 $\pm$ 46.2	286.0 $\pm$ 62.9
Tyrosine	48.8 $\pm$ 6.5	38.7 $\pm$ 8.6	47.3 $\pm$ 8.5	49.7 $\pm$ 13.2
Uridine	49.4 $\pm$ 7.2	50.1 $\pm$ 12.3	48.7 $\pm$ 11.2	50.3 $\pm$ 12.7
Valine	73.5 $\pm$ 9.5	64.4 $\pm$ 13.2	62.6 $\pm$ 9.2	62.6 $\pm$ 12.6
Myo-Inositol	3604.2 $\pm$ 500.5	3660.0 $\pm$ 696.7	4312.7 $\pm$ 551.3	4252.8 $\pm$ 835.1
sn-Glycero-3-phosphocholine	81.1 $\pm$ 11.3	361.0 $\pm$ 82.6	106.8 $\pm$ 14.6	350.5 $\pm$ 68.9
3-Methylhistidine	32.7 $\pm$ 4.6	32.3 $\pm$ 4.7	36.6 $\pm$ 5.6	43.5 $\pm$ 7.6

<sup>b</sup> Difference between AC vs YC groups<sup>c</sup> Difference between AL vs AC groups ( $p < 0.05$ ; two-way ANOVA, followed by the Bonferroni post hoc analysis)

genes for excitatory neurotransmitters [52]. Therefore, the metabolomics results are consistent with a mechanism of brain photobiomodulation of cytochrome-c-oxidase coupled to the transcriptional regulation of nuclear respiratory factor genes, which in turn are coupled with transcription of excitatory neurotransmitter receptors, such as NMDA receptor subunit genes for glutamatergic excitatory neurotransmission [50].

### Photobiomodulation Restores the Brain Metabolic Pathways of Aged Rats Towards the Levels of Younger Rats

On the other hand, in aged rats, we found an opposite effect induced by photobiomodulation. We noted reductions of brain metabolites when comparing AC and AL groups. For example, photobiomodulation decreased cortical levels of

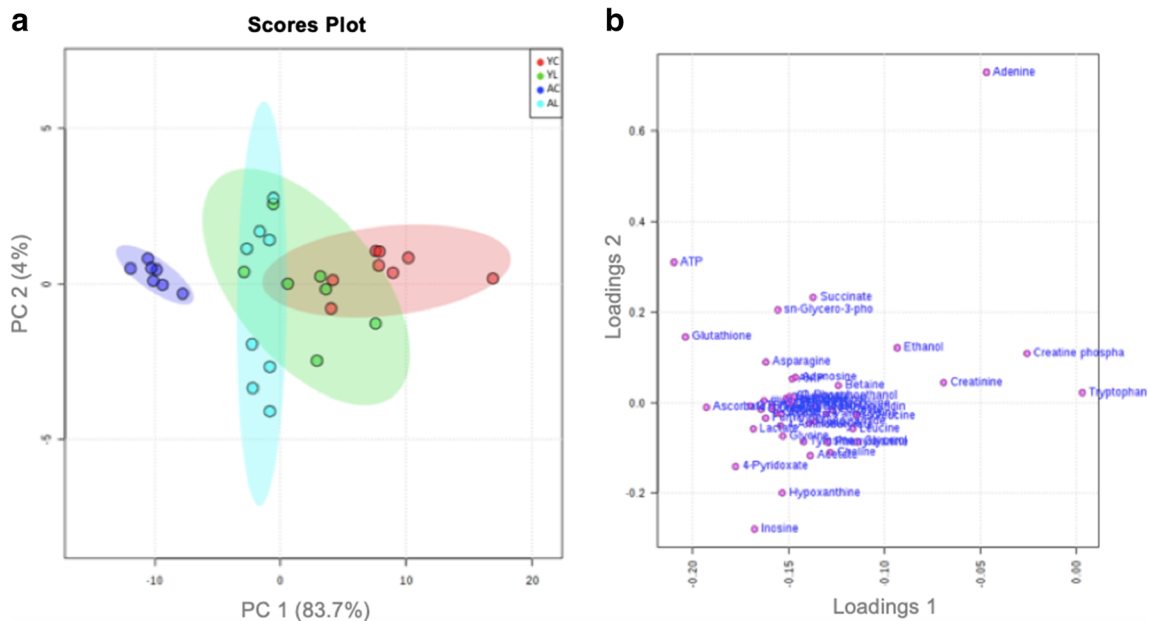


**Fig. 2** Effect of photobiomodulation on cortical PCA from YC (in red;  $n = 8$ ), YL (in green;  $n = 7$ ), AC (in blue;  $n = 7$ ) and AL (in turquoise;  $n = 8$ ) groups. Score plot (a) and loading plot (b) of the PCA by online metabolomics platform MetaboAnalyst

phenylalanine, purines, phosphatidylcholine, and tyrosine in aged rats. Perhaps this photobiomodulation-induced effect on

the aged brain might not be negative, because exacerbated levels of these molecules are linked to phenylketonuria,

**Fig. 3** Cortical metabolic pathways altered by photobiomodulation in young rats (YC vs YL), generated by the online metabolic platform MetaboAnalyst

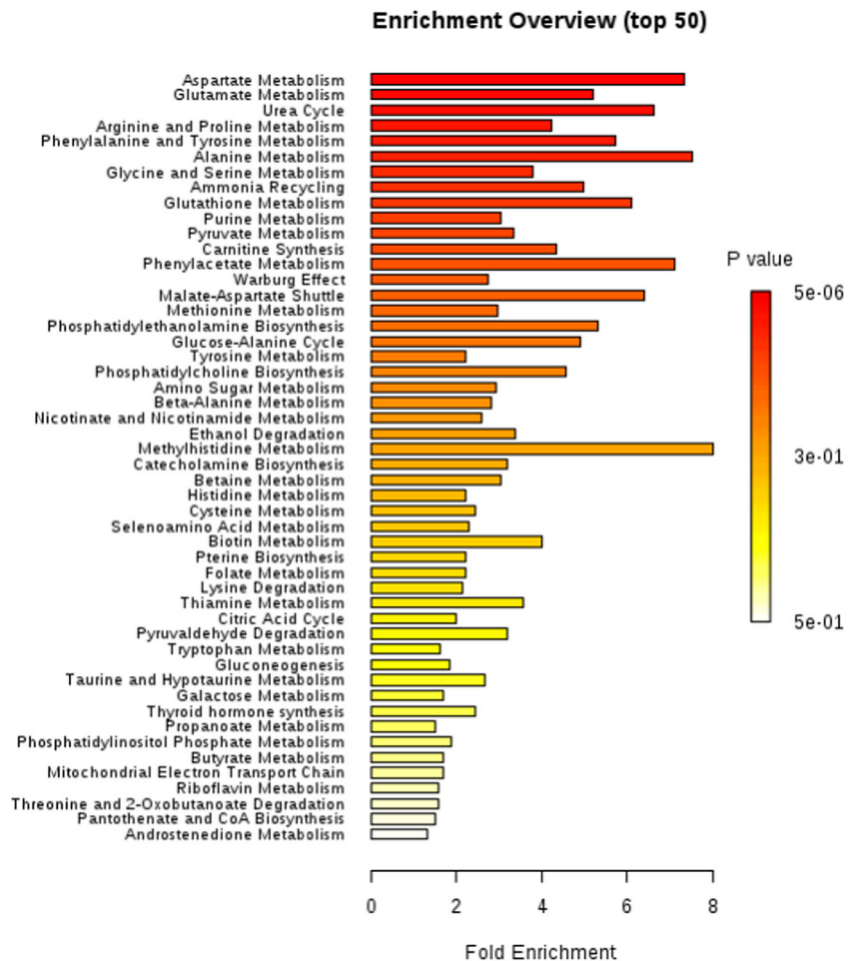
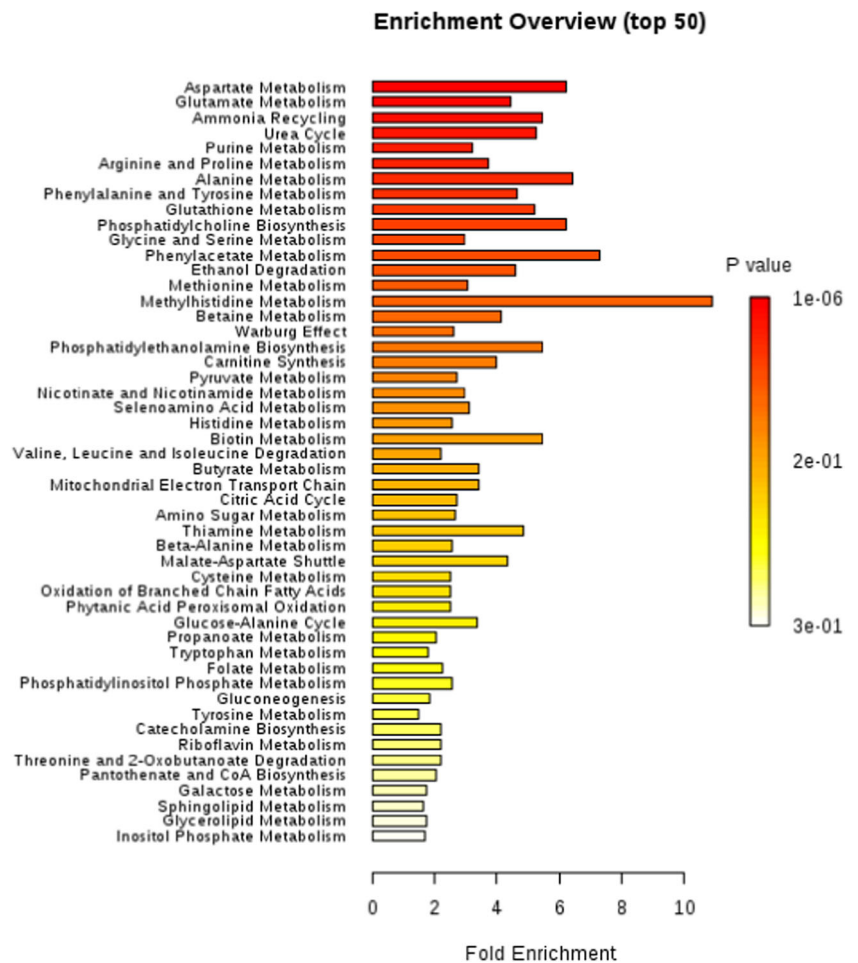




**Fig. 4** Cortical metabolic pathways altered by photobiomodulation in aged rats (AC vs AL), generated by the online metabolic platform MetaboAnalyst



tyrosinemia type II, and other diseases [53–56]. Furthermore, in the brains of older patients with Alzheimer’s disease, the metabolism of purines is deregulated, triggering oxidative

stress [57, 58]. Deregulated metabolism of purines alters signaling and results in neuronal degeneration [59]. Moreover, it is known that high metabolites involved in the purine

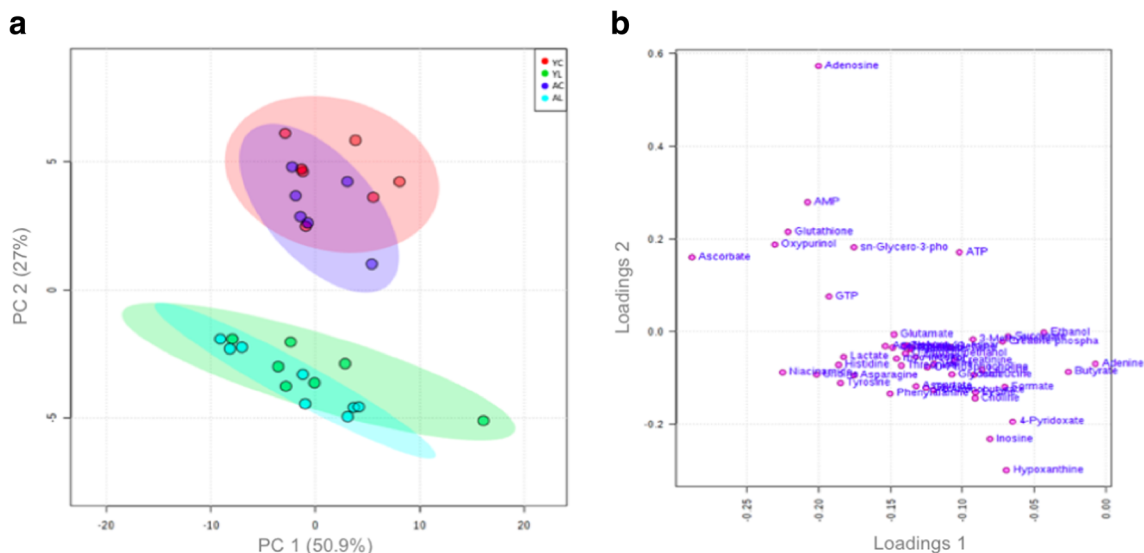
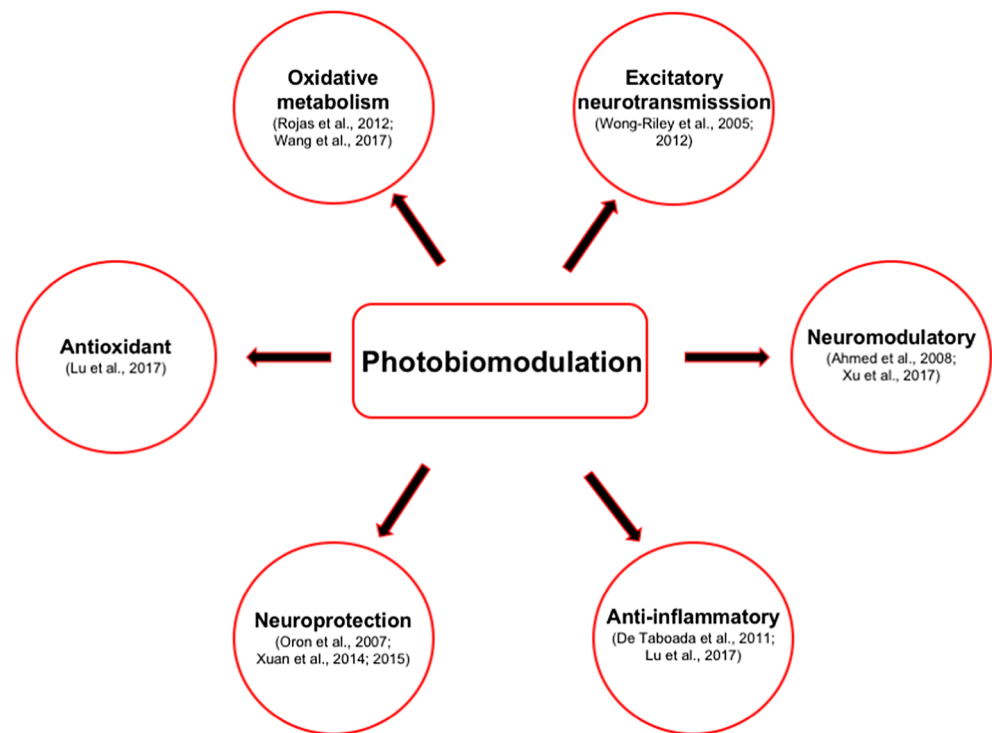


**Fig. 5** Effect of photobiomodulation on hippocampal PCA from YC (in red;  $n = 7$ ), YL (in green;  $n = 7$ ), AC (in blue;  $n = 6$ ), and AL (in turquoise;  $n = 8$ ) groups. Score plot (a) and loading plot (b) of the PCA by online metabolomics platform MetaboAnalyst

**Fig. 6** Various effects of photobiomodulation on the brain



metabolic pathway such as AMP contributes to an increase in ammonia production [60] and disruption of the urea cycle (metabolic pathways that were increased in aged animals), triggering neurological disorders [61].

Photobiomodulation also reduced the phosphatidylcholine biosynthesis pathway in cerebral cortex from aged rats. During aging, phosphatidylcholine biosynthesis influences the activity of enzymes that contribute to amyloid deposition [62], synaptic dysfunction, cell death, and cognitive impairment [63]. Supporting other potential positive effects of photobiomodulation during aging, photobiomodulation reduced the metabolic pathways of aspartate, glutamate, arginine, proline, alanine, glycine, serine, and glutathione. These data are promising, since high levels of these molecules have been related to excitotoxicity and Alzheimer's disease. For example, excess aspartate and glutamate causes ionic imbalance, by an excessive input of sodium and calcium ions, resulting in neuronal death [64–67]. High levels of proline promote inhibition of Na<sup>+</sup>, K<sup>+</sup>-ATPase activity from rat hippocampus [68]. Increased concentration of alanine, glycine, and serine in specific regions of the brain has been associated with beta amyloid deposition and neurofibrillary tangles [69].

In our study, photobiomodulation reduced elevated levels of the cortical metabolic pathway of glutathione in aged rats. This was surprising because we expected a photobiomodulation-induced increase in the cortical metabolic pathway of glutathione in aged rats, as demonstrated in studies of caloric restriction [70, 71]. Possibly these results are related to increased levels of

glutamate and glycine, metabolites responsible for glutathione synthesis [72].

Our results showed that photobiomodulation altered the cortical metabolic pathways of healthy young and aged rats, whereas they showed little effects on hippocampal metabolites (e.g., laser only increased the concentration of acetate and GTP of aged rats). However, a laser-induced increase of GTP in the aged hippocampus is important because GTP is one of the building blocks needed for RNA synthesis and serves as a source of energy during protein synthesis [73]. Furthermore, beneficial photobiomodulation effects have been described in the hippocampus of rodent models with excessive beta amyloid or brain injury. For example, photobiomodulation was able to reduce the amount of beta amyloid plaques, improve mitochondrial function, and restore inflammatory levels in the hippocampus of transgenic mice overexpressing beta amyloid [15] and after injection of beta amyloid directly into the hippocampus of rats [74]. In addition, Xuan et al. [75, 76] noted that photobiomodulation reduces inflammatory levels and promotes hippocampal neurogenesis after traumatic brain injury in mice. Despite these findings in lesion models, our data showing predominantly cortical as compared to hippocampal effects are consistent with the results of Xu et al. [77]. They noted that when they used photobiomodulation to treat mice in a depression model, these mice exhibited a greater synthesis of cortical ATP. However, this effect was not observed in the hippocampus of these animals. Better consistency of the brain regions that could be altered by photobiomodulation in

rodents requires a standard irradiation protocol given under similar conditions, since the literature shows very different protocols and conditions.

## Limitations

This is the first study to investigate photobiomodulation effects on metabolomics *in vivo*, so other questions remain to be investigated. For example, this paper did not evaluate functional parameters, such as cognitive functions, since our only purpose was to investigate whether this laser treatment alters the cortical and hippocampal metabolic profiles in young and aged rats. Functional tests are still lacking in the literature, and it is our next target to analyze functional tasks in future cognitive studies. The use of one dose is also a limitation of this study. We used only one dose due to the difficulty in obtaining aged rats. This dose was used based on our previous studies showing anti-inflammatory effects. A homogeneous trend of metabolite change leaves the possibility of systematic analytical bias. We recognize that this bias exists, but it is inherent in the NMR technique.

## Conclusions

Taken together, our novel metabolomics data indicate that transcranial photobiomodulation (1) increases the brain metabolic pathways of young rats, particularly for cortical excitatory neurotransmission and oxidative metabolism, and (2) restores the brain metabolic pathways of aged rats towards the levels of younger rats. The present metabolic profiles implicating cortical excitatory neurotransmission and oxidative metabolism related to cytochrome-c-oxidase [12, 51, 52] can serve to complement other photobiomodulation-induced neuroprotective, neuromodulatory, anti-inflammatory, and antioxidant effects described in the literature [14, 15, 50, 74, 77, 78]. Figure 6 provides a “big picture” schematic summarizing these overall benefits of transcranial photobiomodulation.

**Supplementary Information** The online version contains supplementary material available at <https://doi.org/10.1007/s12035-020-02247-z>.

**Acknowledgments** We thank the Nuclear Magnetic Resonance (NMR) Facility at Brazilian Biosciences National Laboratory (LNBio) and Brazilian Center for Research in Energy and Materials (CNPEM) for the use of the NMR spectrometer.

**Authors' Contributions** All authors read and approved the final manuscript.

**Funding** This study was supported by Coordenação de Aperfeiçoamento de Pessoal de Nível Superior (CAPES), Centros de Pesquisa, Inovação e Difusão (CEPID; 2013/08028-1 and Fundação de Amparo à Pesquisa do Estado de São Paulo (FAPESP; #2017/16443-0). Francisco Gonzalez-Lima was supported by the Oskar Fischer Project Fund. Rodrigo Álvaro Brandão Lopes-Martins was supported by the Conselho

Nacional de Desenvolvimento Científico e Tecnológico (CNPq; 307839/2015-0).

## Compliance with Ethical Standards

**Conflict of Interest** The authors declare that they have no conflicts of interest.

## References

- Anders JJ, Lanzafame RJ, Arany PR (2015) Low-level light/laser therapy versus photobiomodulation therapy. *Photomed Laser Surg* 33:183–184
- Arany PR (2016) Craniofacial wound healing with photobiomodulation therapy: new insights and current challenges. *J Dent Res* 95:977–984
- Chung H, Dai T, Sharma SK, Huang YY, Carroll JD, Hamblin MR (2012) The nuts and bolts of low-level laser (light) therapy. *Ann Biomed Eng* 40:516–533
- Eells JT, Wong-Riley MT, VerHoeve J, Henry M, Buchman EV, Kane MP, Gould LJ, Dias R et al (2004) Mitochondrial signal transduction in accelerated wound and retinal healing by near-infrared light therapy. *Mitochondrion* 4:559–567
- Rojas JC, Gonzalez-Lima F (2011) Low-level light therapy of the eye and brain. *Eye Brain* 3:49–67
- Shinmar H, Grewal M, Sivaprasad S, Hogg C, Chong V, Neveu M, Jeffery G (2020) Optically improved mitochondrial function redeems aged human visual decline. *J Gerontol Ser A* 75:e49–e52
- Wong-Riley MT, Liang HL, Eells JT, Chance B, Henry MM, Buchmann E, Kane M, Whelan HT (2005) Photobiomodulation directly benefits primary neurons functionally inactivated by toxins: role of cytochrome c oxidase. *J Biol Chem* 280:4761–4771
- Holanda VM, Chavantes MC, Wu X, Anders JJ (2017) The mechanistic basis for photobiomodulation therapy of neuropathic pain by near infrared laser light. *Lasers Surg Med* 49:516–524
- El Khoury H, Mitrofanis J, Henderson LA (2019) Exploring the effects of near infrared light on resting and evoked brain activity in humans using magnetic resonance imaging. *Neuroscience* 422: 161–171
- Mitrofanis J, Henderson LA (2020) How and why does photobiomodulation change brain activity? *Neural Regen Res* 15: 2243–2244
- Rojas JC, Gonzalez-Lima F (2013) Neurological and psychological applications of transcranial lasers and LEDs. *Biochem Pharmacol* 86:447–457
- Wang X, Tian F, Reddy DD, Nalawade SS, Barrett DW, Gonzalez-Lima F, Liu H (2017) Up-regulation of cerebral cytochrome-c-oxidase and hemodynamics by transcranial infrared laser stimulation: a broadband near-infrared spectroscopy study. *J Cereb Blood Flow Metab* 37:3789–3802
- Wang X, Dmochowski JP, Zeng L, Kallioniemi E, Husain M, Gonzalez-Lima F, Liu H (2019) Transcranial photobiomodulation with 1064-nm laser modulates brain electroencephalogram rhythms. *Neurophotonics* 6:025013
- Oron A, Oron U, Streeter J, Taboada L, Alexandrovich A, Trembovler V, Shohami E (2007) Low-level laser therapy applied transcranially to mice following traumatic brain injury significantly reduces long-term neurological deficits. *J Neurotrauma* 24:651–656
- De Taboada L, Yu J, El-Amouri S, Gattoni-Celli S, Richieri S, McCarthy T, Kindy MS (2011) Transcranial laser therapy attenuates amyloid- $\beta$  peptide neuropathology in amyloid- $\beta$  protein precursor transgenic mice. *J Alzheimers Dis* 23:521–535

16. Mitrofanis J, Jeffery G (2018) Does photobiomodulation influence ageing? *Aging (Albany NY)* 10:2224–2225
17. Mattson MP, Magnus T (2006) Ageing and neuronal vulnerability. *Nat Rev Neurosci* 7:278–294
18. Boveris A, Navarro A (2008) Brain mitochondrial dysfunction in aging. *IUBMB Life* 60:308–314
19. Yin F, Boveris A, Cadenas E (2014) Mitochondrial energy metabolism and redox signaling in brain aging and neurodegeneration. *Antioxid Redox Signal* 20:353–371
20. Petit-Taboue MC, Landeau B, Desson JF, Desgranges B, Baron JC (1988) Effects of healthy aging on the regional cerebral metabolic rate of glucose assessed with statistical parametric mapping. *Neuroimage*. 7:176–184
21. Miccheli A, Puccetti C, Capuani G, Di Cocco ME, Giardino L, Calzà L, Bettaglia A, Battistin L et al (2003) [1-13C] Glucose entry in neuronal and astrocytic intermediary metabolism of aged rats: a study of the effects of nicergoline treatment by 13C NMR spectroscopy. *Brain Res* 966:116–125
22. Martínez A, Portero-Otin M, Pamplona R, Ferrer I (2010) Protein targets of oxidative damage in human neurodegenerative diseases with abnormal protein aggregates. *Brain Pathol* 20:281–297
23. Dubey A, Forster MJ, Lal H, Sohal RS (1996) Effect of age and caloric intake on protein oxidation in different brain regions and on behavioral functions of the mouse. *Arch Biochem Biophys* 333:189–197
24. Lu T, Pan Y, Kao SY, Li C, Kohane I, Chan J, Yankner BA (2004) Gene regulation and DNA damage in the ageing human brain. *Nature*. 429:883–891
25. Butterfield DA, Perluigi M, Reed T, Muharib T, Hughes CP, Robinson RA, Sultana R (2012) Redox proteomics in selected neurodegenerative disorders: from its infancy to future applications. *Antioxid Redox Signal* 17:1610–1655
26. Vargas E, Barrett DW, Saucedo CL, Huang LD, Abraham JA, Tanaka H, Haley AP, Gonzalez-Lima F (2017) Beneficial neurocognitive effects of transcranial laser in older adults. *Lasers Med Sci* 32:1153–1162
27. Wang TJ, Larson MG, Vasan RS, Cheng S, Rhee EP, McCabe E, Lewis GD, Fox CS et al (2011) Metabolite profiles and the risk of developing diabetes. *Nat Med* 17:448–453
28. Xia J, Sinelnikov IV, Han B, Wishart DS (2015) MetaboAnalyst 3.0—making metabolomics more meaningful. *Nucleic Acids Res* 43:W251–W257
29. CIOMS (1985) International guiding principles for biomedical research involving animals. *Altern Lab Anim* 12:ii
30. Paxinos G, Watson C (2006) The rat brain in stereotaxic coordinates. Ed 6. Academic, Amsterdam
31. Almeida P, Lopes-Martins RÁ, Tomazoni SS, Albuquerque-Pontes GM, Santos LA, Vanin AA, Frigo L, Vieira RP et al (2013) Low-level laser therapy and sodium diclofenac in acute inflammatory response induced by skeletal muscle trauma: effects in muscle morphology and mRNA gene expression of inflammatory markers. *Photochem Photobiol* 89:501–507
32. Haslerud S, Lopes-Martins RA, Frigo L, Bjordal JM, Marcos RL, Naterstad IF, Magnussen LH, Joensen J (2017) Low-level laser therapy and cryotherapy as mono- and adjunctive therapies for Achilles tendinopathy in rats. *Photomed Laser Surg* 35:32–42
33. Naterstad IF, Rossi RP, Marcos RL, Parizzoto NA, Frigo L, Joensen J, Lopes Martins PSL, Bjordal JM et al (2018) Comparison of photobiomodulation and anti-inflammatory drugs on tissue repair on collagenase-induced Achilles tendon inflammation in rats. *Photomed Laser Surg* 36:137–145
34. Tomazoni SS, Leal-Junior EC, Pallotta RC, Teixeira S, de Almeida P, Lopes-Martins RÁ (2017) Effects of photobiomodulation therapy, pharmacological therapy, and physical exercise as single and/or combined treatment on the inflammatory response induced by experimental osteoarthritis. *Lasers Med Sci* 32:101–108
35. Morries LD, Cassano P, Henderson TA (2015) Treatments for traumatic brain injury with emphasis on transcranial near-infrared laser phototherapy. *Neuropsychiatr Dis Treat* 11:2159–2175
36. Henderson TA, Morries LD (2015) Near-infrared photonic energy penetration: can infrared phototherapy effectively reach the human brain? *Neuropsychiatr Dis Treat* 11:2191–2208
37. Carreras AL, Mattos-Dutra A, Meirelles R, Rocha BB, Wannmacher CMD, Pessoa-Pureur R (2000) Phenylalanine inhibition of the phosphorylation of cytoskeletal proteins from cerebral cortex of young rats is prevented by alanine. *Eur J Clin Investig* 30:536–542
38. Katsuki H, Watanabe Y, Fujimoto S, Kume T, Akaike A (2007) Contribution of endogenous glycine and d-serine to excitotoxic and ischemic cell death in rat cerebrocortical slice cultures. *Life Sci* 81:740–749
39. Meldrum BS (2000) Glutamate as a neurotransmitter in the brain: review of physiology and pathology. *J Nutr* 130:1007S–1015S
40. Stefanic P, Dolenc MS (2004) Aspartate and glutamate mimetic structures in biologically active compounds. *Curr Med Chem* 11:945–968
41. Ault B, Wang CM, Yawn BC (1987) L-proline depolarizes rat spinal motoneurons by an excitatory amino acid antagonist-sensitive mechanism. *Br J Pharmacol* 92:319–326
42. Henzi V, Reichling DB, Helm SW, MacDermott AB (1992) L-proline activates glutamate and glycine receptors in cultured rat dorsal horn neurons. *Mol Pharmacol* 41:793–801
43. Martin D, Ault B, Nadler JV (1992) NMDA receptor-mediated depolarizing action of proline on CA1 pyramidal cells. *Eur J Pharmacol* 219:59–66
44. Pace JR, Brian M, Paul SM, Rogawski MA (1992) High concentrations of neutral amino acids activate NMDA receptor currents in rat hippocampal neurons. *Neurosci Lett* 141:97–100
45. Konstantinović LM, Jelić MB, Jeremić A, Stevanović VB, Milanović SD, Filipović SR (2013) Transcranial application of near-infrared low-level laser can modulate cortical excitability. *Lasers Surg Med* 45:648–653
46. Aoyama K, Nakaki T (2015) Glutathione in cellular redox homeostasis: association with the excitatory amino acid carrier 1 (EAAC1). *Molecules*. 20:8742–8758
47. Rae CD, Williams SR (2017) Glutathione in the human brain: review of its roles and measurement by magnetic resonance spectroscopy. *Anal Biochem* 529:127–143
48. Puig MV, Antzoulatos EG, Miller EK (2014) Prefrontal dopamine in associative learning and memory. *Neuroscience*. 282:217–229
49. Shnitko TA, Taylor SC, Stringfield SJ, Zandy SL, Cofresí RU, Doherty JM, Lynch WB, Boettiger CA et al (2016) Acute phenylalanine/tyrosine depletion of phasic dopamine in the rat brain. *Psychopharmacology*. 233:2045–2054
50. Rojas JC, Gonzalez-Lima F (2017) Transcranial low-level laser light therapy for neurocognitive enhancement. In: Hamblin MR, Sousa MV, Agrawal T (eds) *Handbook of low-level laser therapy*. Pan Stanford Publishing, Singapore, pp. 1057–1076
51. Rojas JC, Bruchey AK, Gonzalez-Lima F (2012) Low-level light therapy improves cortical metabolic capacity and memory retention. *J Alzheimers Dis* 32:741–752
52. Wong-Riley MT (2012) Bigenomic regulation of cytochrome c oxidase in neurons and the tight coupling between neuronal activity and energy metabolism. *Adv Exp Med Biol* 748:283–304
53. Banik D, Kundu S, Banerjee P, Dutta R, Sarkar N (2017) Investigation of fibril forming mechanisms of l-phenylalanine and l-tyrosine: microscopic insight toward phenylketonuria and tyrosinemia type II. *J Phys Chem B* 121:1533–1543
54. Blau N, van Spronsen FJ, Levy HL (2010) Phenylketonuria. *Lancet* 376:1417–1427



55. Francis DEM, Kirby DM, Thompson GN (1992) Maternal tyrosinaemia II: management and successful outcome. *Eur J Pediatr* 151:196–199
56. Huttenlocher PR (2000) The neuropathology of phenylketonuria: human and animal studies. *Eur J Pediatr* 159:S102–S106
57. Gabbita SP, Lovell MA, Markesbery WR (1998) Increased nuclear DNA oxidation in the brain in Alzheimer's disease. *J Neurochem* 71:2034–2040
58. Lyras L, Cairns NJ, Jenner A, Jenner P, Halliwell B (1997) An assessment of oxidative damage to proteins, lipids, and DNA in brain from patients with Alzheimer's disease. *J Neurochem* 68:2061–2069
59. Abbracchio MP, Burnstock G (1998) Purinergic signalling: pathophysiological roles. *Jpn J Pharmacol* 78:113–145
60. Sims B, Powers RE, Sabina RL, Theibert AB (1998) Elevated adenosine monophosphate deaminase activity in Alzheimer's disease brain. *Neurobiol Aging* 19:385–391
61. Matsumoto S, Häberle J, Kido J, Mitsubuchi H, Endo F, Nakamura K (2019) Urea cycle disorders—update. *J Hum Genet* 64:833–847
62. Holmes O, Paturi S, Ye W, Wolfe MS, Selkoe DJ (2012) Effects of membrane lipids on the activity and processivity of purified  $\gamma$ -secretase. *Biochemistry*. 51:3565–3575
63. Ledesma MD, Martin MG, Dotti CG (2012) Lipid changes in the aged brain: effect on synaptic function and neuronal survival. *Prog Lipid Res* 51:23–35
64. Choi DW (1988) Glutamate neurotoxicity and diseases of the nervous system. *Neuron*. 1:623–634
65. Du Y, Bales KR, Dodel RC, Hamilton-Byrd E, Horn JW, Czilli DL, Simmons LK, Ni B et al (1997) Activation of a caspase 3-related cysteine protease is required for glutamate-mediated apoptosis of cultured cerebellar granule neurons. *Proc Natl Acad Sci* 94:11657–11662
66. Nicholls D, Attwell D (1990) The release and uptake of excitatory amino acids. *Trends Pharmacol Sci* 11:462–468
67. Rush T, Liu X, Lobner D (2012) Synergistic toxicity of the environmental neurotoxins methylmercury and  $\beta$ -N-methylamino-L-alanine. *Neuroreport*. 23:216–219
68. Pontes ZL, Oliveira LS, Franzon R, Wajner M, Wannmacher CMD, Souza Wyse AT (2001) Inhibition of Na<sup>+</sup>, K<sup>+</sup>-ATPase activity from rat hippocampus by proline. *Neurochem Res* 26:1321–1326
69. An Y, Varma VR, Varma S, Casanova R, Dammer E, Pletnikova O, Chia CW, Egan JM et al (2018) Evidence for brain glucose dysregulation in Alzheimer's disease. *Alzheimers Dement* 14:318–329
70. Rebrin I, Kamzalov S, Sohal RS (2003) Effects of age and caloric restriction on glutathione redox state in mice. *Free Radic Biol Med* 35:626–635
71. Rebrin I, Forster MJ, Sohal RS (2007) Effects of age and caloric intake on glutathione redox state in different brain regions of C57BL/6 and DBA/2 mice. *Brain Res* 1127:10–18
72. Wu G, Fang YZ, Yang S, Lupton JR, Turner ND (2004) Glutathione metabolism and its implications for health. *J Nutr* 134:489–492
73. Wallin G, Kamerlin SC, Åqvist J (2013) Energetics of activation of GTP hydrolysis on the ribosome. *Nat Commun* 4:1–10
74. Lu Y, Wang R, Dong Y, Tucker D, Zhao N, Ahmed ME, Zhu L, Liu TCY et al (2017) Low-level laser therapy for beta amyloid toxicity in rat hippocampus. *Neurobiol Aging* 49:165–182
75. Xuan W, Vatanserver F, Huang L, Hamblin MR (2014) Transcranial low-level laser therapy enhances learning, memory, and neuroprogenitor cells after traumatic brain injury in mice. *J Biomed Opt* 19:108003
76. Xuan W, Agrawal T, Huang L, Gupta GK, Hamblin MR (2015) Low-level laser therapy for traumatic brain injury in mice increases brain derived neurotrophic factor (BDNF) and synaptogenesis. *J Biophotonics* 8:502–511
77. Xu Z, Guo X, Yang Y, Tucker D, Lu Y, Xin N, Zhang Q (2017) Low-level laser irradiation improves depression-like behaviors in mice. *Mol Neurobiol* 54:4551–4559
78. Ahmed NAEH, Radwan NM, Ibrahim KM, Khedr ME, El Aziz MA, Khadrawy YA (2008) Effect of three different intensities of infrared laser energy on the levels of amino acid neurotransmitters in the cortex and hippocampus of rat brain. *Photomed Laser Surg* 26:479–488

**Publisher's Note** Springer Nature remains neutral with regard to jurisdictional claims in published maps and institutional affiliations.